Hiroshi Yoshihara* and Masahiro Yoshinobu

In-plane shear strength of paper measured by asymmetric four-point bending test

Abstract: The in-plane shear strengths (IPSS) of copy paper, filter paper, and sack paper were obtained from an asymmetric four-point bending (AFPB) test. Rectangular tabs of medium-density fibreboard (MDF) were bonded to the paper specimen. The length of the clearance between the tabs was varied, and the influence of the clearance on the IPSS value was investigated. The IPSS obtained from the AFPB test was compared with that obtained from a 35° off-axis tension (OAT) test, which was proposed in a previous study. The IPSS values obtained from the AFPB tests on the copy paper and sack paper were significantly lower than those obtained from the 35° OAT tests because of the localised buckling caused by the negative principal stress. In contrast, the IPSS values obtained from the AFPB and OAT tests on the filter paper were in agreement when the clearance length was >5 mm because the buckling effect was excluded.

Keywords: asymmetric four-point bending test, clearance, finite element analysis (FEA), in-plane shear strength, off-axis tension test, paper

DOI 10.1515/hf-2014-0047
Received February 14, 2014; accepted April 10, 2014; previously published online May 15, 2014

Introduction

The mechanical properties of papers as packaging material and in containers, including the in-plane shear strength (IPSS), must be determined reliably for effective utilisation. Several studies focused on the IPSS of paper through simple shear (SS) tests (Fellers 1977; Heckers and Göttsching 1980; Waterhouse 1984; Pan and Zhang 1997), but there are no established methods for measuring the IPSS of paper.

Off-axis tension (OAT) tests of several papers were conducted in a previous study, and an equation for predicting the IPSS of paper was proposed by means of the 35° OAT strength (Yoshihara and Yoshinobu 2014). However, the IPSS was not measured under a pure shear stress condition in the quoted study. The IPSS was roughly estimated based on the concept that the strength properties of paper obey certain Hill-type failure conditions proposed by Norris (1962), Azzi and Tsai (1965), and Wu and Stachurski (1984). Because the experimental conditions were not well examined, the suitability of the method for IPSS determination of paper is not yet validated. A method based on the off-axis loading (OAL) tests was proposed for determining the shear properties including the shear stress-strain relationship, shear modulus, and shear strength of composite materials (Koerber et al. 2010).

Here the OAL test data are regressed into a suitable failure condition in the combined normal and in-plane shear stress state, and the pure IPSS was determined by extrapolating the normal stress component to zero. This method is advantageous in that the shear modulus can be obtained as well as the shear strength. Nevertheless, it requires the angle between the fracture plane and specimen's surface in the thickness direction. Because of the thinness of paper, this angle is difficult to measure. Considering the drawbacks of OAT test, it is more desirable to measure the IPSS by another method. Asymmetric four-point bending (AFPB) tests have been often conducted to measure the IPSS of solid wood and wood-based materials under near pure shear stress conditions (Yoshihara and Suzuki 2005; Yoshihara 2009, 2012; Yoshihara and Kondo 2013). The working hypothesis is that this method may also be applicable for measuring the IPSS of paper.

In this study, AFPB tests were performed on samples of copy paper, filter paper and sack paper. The validity of this method was examined by comparing the results with those obtained from finite element (FE) calculations and the 35° OAT test proposed in the aforementioned study.

***Corresponding author: Hiroshi Yoshihara,** Faculty of Science and Engineering, Shimane University, Nishikawazu-cho 1060, Matsue, Shimane 690-8504, Japan, e-mail: yosihara@riko.shimane-u.ac.jp
Masahiro Yoshinobu: Faculty of Science and Engineering, Shimane University, Nishikawazu-cho 1060, Matsue, Shimane 690-8504, Japan

Table 1 Basis weight, thickness, and density of the test samples.

Paper type	Basis weight (g m⁻²)	Thickness (μm)	Density (kg m⁻³)
Copy p.	70.5±1.2	90±1	805±10
Filter p.	282±6	908±10	310±2
Sack p.	99±2	151±2	700±0.6

Materials and methods

Commercial copy paper, unbleached sack paper, and filter paper, all of which consisted of cellulose, were investigated, and off-axis (OA) specimens were cut from these papers. For each specimen, the basis weight, thickness, and density were measured, and are listed in Table 1. The thickness of each sample was measured according to JIS P8118-98 (1998) with a micrometer (measuring range=0–25 mm, 0.01 mm divisions, PPM-25, Mitsutoyo, Kawasaki, Japan) with a constant pressure of 50 kPa applied by a pair of flat circular ground faces of 14.3 mm in diameter. The specimen was prepared in a climate room (20°C, 65% RH). Ten specimens were prepared for each test condition.

Finite element analysis (FEA): A three-dimensional (3D) FEA was performed prior to the AFPB tests using the FEA program ANSYS 12.0 (2009). Figure 1 presents a diagram of the FE mesh of the model. The side and top views of the model are shown in Figure 1a and b, respectively, whereas the mesh detail is provided in Figure 1c. The model consisted of eight noded brick elements.

A model with a length direction that is coincident with the machine direction (MD) and a model that is coincident with the cross direction (CD) of the paper are defined as an MD and CD models, respectively. For a beam specimen cut from the paper sheet, the MD, CD, and thickness direction are defined as the *M*, *C*, and *z* directions, respectively, whereas the length and depth directions of the specimen were defined as the *x* and *y* directions, respectively. The model had a length of 260 mm. The depth *W* was 40 mm. The width *B*, corresponding to the thickness of the paper, were 0.09 mm (copy paper), 0.9 mm (filter paper), and 0.15 mm (sack paper).

The elastic constants were measured through uniaxial tension tests of rectangular specimens prior to the FEAs. Each specimen had dimensions of 240 mm by 20 mm. To measure the strain in the length direction, two 20 mm straight lines were drawn at the mid-length point. The specimen was clamped with grips at the distance of 180 mm, and a load was applied to the specimen with the cross-head speed of 1.8 mm. The elongation between these lines and the shrinkage of the width were photographed with a CCD camera at

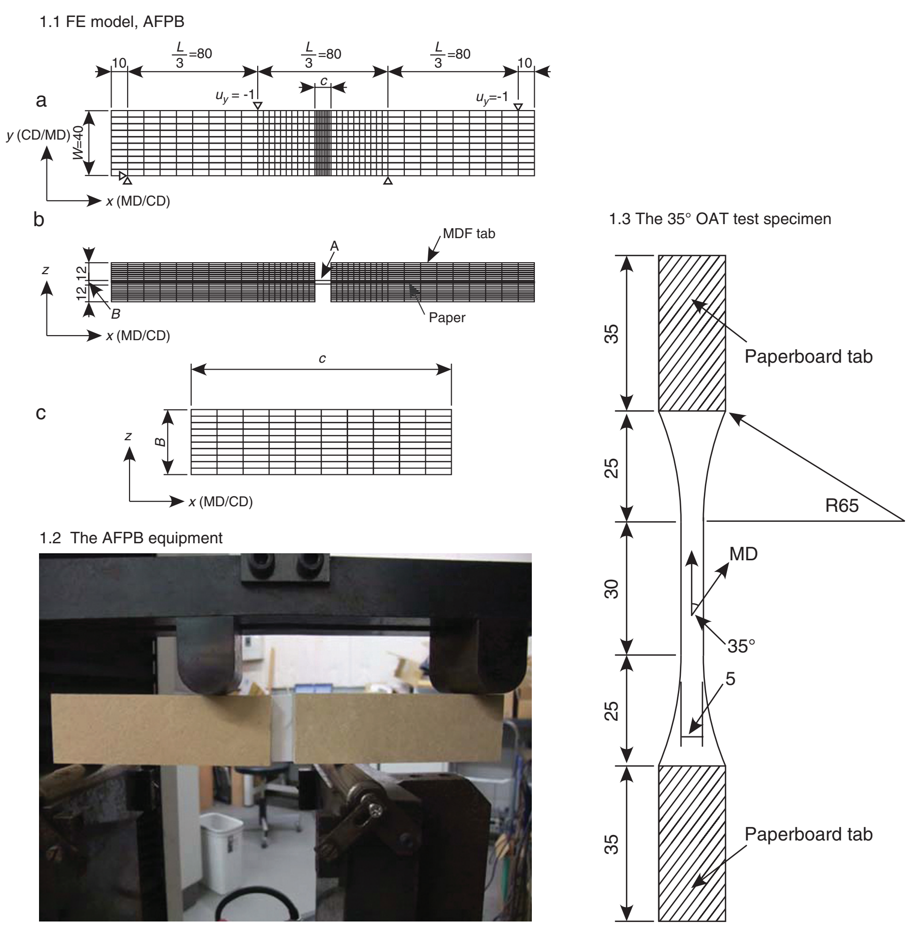

Figure 1 Illustrations of some details of the experiments. **1.1** Finite element (FE) model for the asymmetric four-point bending (AFPB) test of paper in the *xy* and *xz* planes. (a) side view, (b) top view, and (c) detail of Zone A in (b). Unit=mm. **1.2** Photograph of the equipment for AFPB test. **1.3** 35° off-axis tension (OAT) test specimen.

an interval of 0.5 s and analysed by a high-speed digital image sensor (Keyence CV-5000SO, Keyence Corporation, Osaka, Japan); the length and transverse strains were obtained from these elongations. The Young's modulus in the M direction (E_M) and Poisson's ratio in the MC plane (ν_{MC}) were obtained by using the specimen whose length direction coincided with the machine direction. The Young's modulus in the C direction, E_C, was obtained from the specimen the length direction of which coincided with the CD. Based on the specimen with the OA angle of 45°, the shear modulus in the MC plane, G_{MC}, was obtained (Eq. 1):

$$G_{MC}=\frac{E_{45}}{2(1+\nu_{45})} \tag{1}$$

where E_{45} and ν_{45} are the OA Young's modulus and Poisson's ratio of the specimen with the OA angle of 45°. The elastic constants of the papers obtained from the tension tests are listed in Table 2. In the 3D-FEA, the Young's modulus in the z direction, E_z, and the Poisson's ratio and shear modulus in the Mz, and Cz plane, i.e., ν_{Mz}, ν_{Cz}, G_{Mz}, and G_{Cz}, are required. Because it was difficult to measure these values, they were derived as $E_z=E_C$, $\nu_{Mz}=\nu_{Cz}=\nu_{MC}$, and $G_{Mz}=G_{Cz}=G_{MC}$ in these analyses. The elastic constants were obtained based on the concept that the stress and strain are distributed homogeneously in the gauge region (Yoshihara et al. 1998, 1999; Kubojima et al. 2000). It should also be noted that these elastic constants were also determined based on non-uniform state of stress/strain at the gauge section (Xavier et al. 2007, 2009, 2013).

It is difficult to conduct AFPB tests on paper without bonding any tabs to the paper specimen because of its thinness. Therefore, four rectangular tabs of medium-density fiberboard (MDF) with a thickness of 12 mm were bonded on both ends of the specimen in the actual AFPB test. Yoshihara (2011, 2013) assumed that MDF is isotropic, so the Young's modulus, Poisson's ratio, and shear modulus of the MDF applied in the present calculations were 3.2 GPa, 0.36, and 1.18 GPa, respectively.

The clearance between the tab edges was defined as c. Similar to the actual AFPB test, the c value was varied from 0 to 20 mm in 5-mm increments. As illustrated in Figure 1a, the node corresponding to the locations at x=10 and 170 mm of the bottom surface were constrained, and a vertical displacement (u_Y) of 1 mm was applied downward to the nodes corresponding to the locations at x=90 and 250 mm of the top surface. Therefore, the span length L was 240 mm. The total load P was obtained from the nodal forces at the loading points, whereas the shear strain was determined from the node at the neutral axis of the mid-length of the surface element. The IPSS at the neutral axis in the mid-span τ_{xy}^{EBT} was calculated by substituting P into Eq. 2, which is derived based on the elementary beam theory:

$$\tau_{xy}^{\mathrm{EBT}}=\frac{3P}{4BW} \tag{2}$$

Table 2 Elastic constants obtained by the uniaxial-tension tests of each paper.

Paper type	E_M (GPa)	E_C (GPa)	ν_{MC}	G_{MC} (GPa)
Copy p.	5.24±0.94	3.50±0.11	0.30±0.07	1.72±0.37
Filter p.	0.47±0.05	0.29±0.01	0.29±0.03	0.15±0.04
Sack p.	4.15±0.80	1.80±0.17	0.10±0.02	0.95±0.15

$E_C=E_z$, $\nu_{Mz}=\nu_{Cz}=\nu_{MC}$, and $G_{Mz}=G_{Cz}=G_{MC}$.

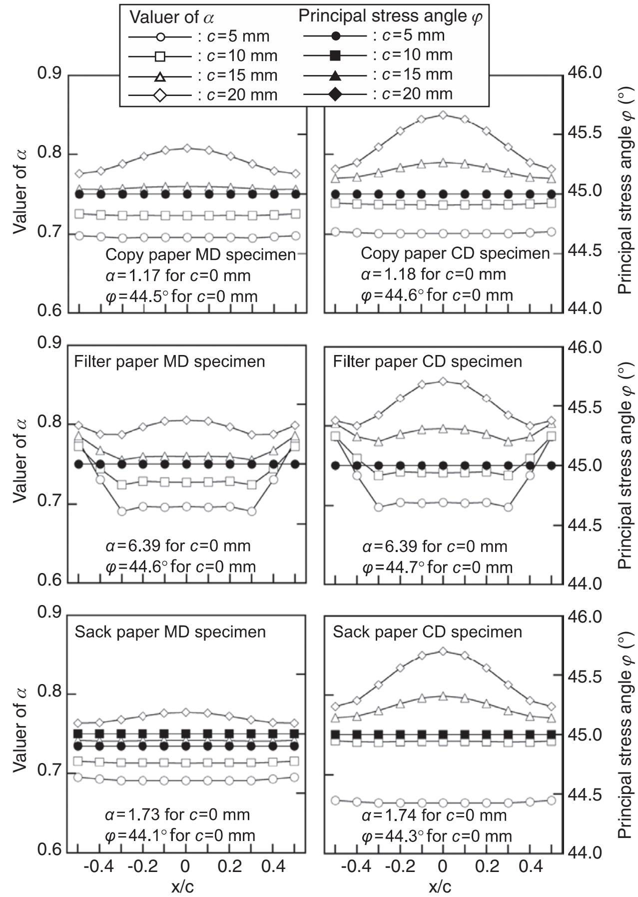

Figure 2 Values of α obtained from the FEAs along the neutral axis corresponding to the location from the mid-length of the model/clearance length x/c.

In contrast, the values of shear stress at the nodes located at the neutral axis in the clearance τ_{xy}^{FEM} were obtained and compared with the τ_{xy}^{EBT} value. It was confirmed that the mesh size was fine enough and the effect of mesh size could be ignored.

AFPB test: The specimens consisted of rectangular strips with dimensions of 260 (x) ×40 (y) mm^2. As previously noted, the x and y axes coincided with the MD (M direction) and CD (C direction), respectively, or vice versa. Figure 2 shows a photograph of the AFPB test. Four rectangular tabs of MDF with a thickness of 12 mm were bonded on the specimen with a double-sided tape. In preparing the AFPB specimen, the clearance between the tabs, shown as c in this figure, was varied from 0 to 20 mm at intervals of 5 mm.

The specimen was asymmetrically supported and loaded (Figure 1). Before loading, the specimen was set so that the tab-free portion was at mid-span. The total span length L was 240 mm, and the specimen was eccentrically supported at two trisected points (x=0 and 160 mm). The load P was applied to the remaining two trisected points (x=80 and 240 mm) at a crosshead speed of 1 mm min^{-1} in the larger and smaller specimens, respectively, until the load markedly decreased.

35° OAT test: Independently of the AFPB tests, 35° OAT tests were also conducted and the shear strengths obtained were compared with those from the AFPB tests. The specimen with the OA angle of 35° with respect to the MD was cut into the dog-boned shape shown in Figure 3. Paperboard tabs (0.7 mm thick) were bonded to each end

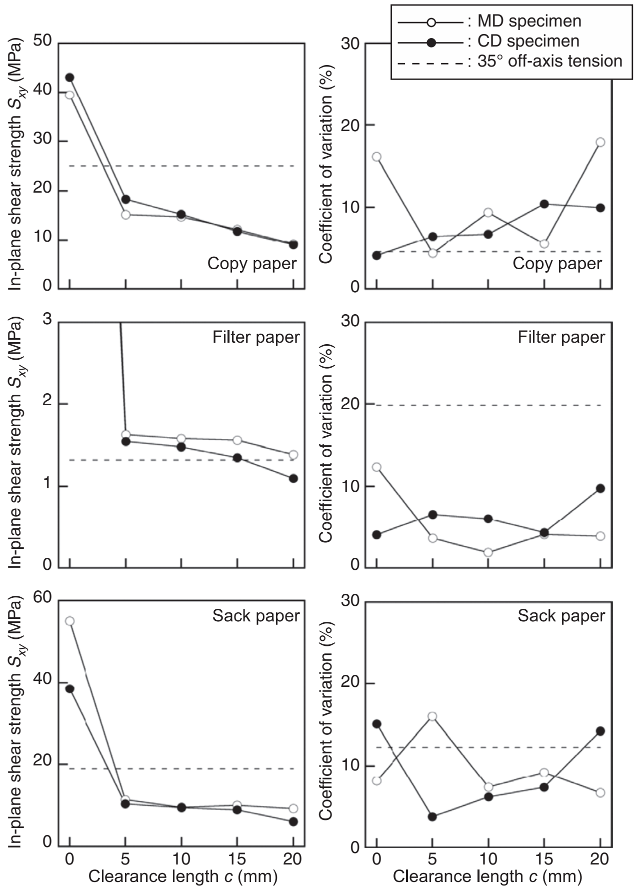

Figure 3 Data of the in-plane shear strength S_{xy} obtained from the AFPB test corresponding to the clearance length c and comparison with that obtained from the 35° OAT test.

of the dog-bone-shaped specimen with double-sided tape to avoid stress concentration at the grips. The specimen was loaded by means of universal tension test fixtures. The tension load was applied at a crosshead speed of 1 mm min^{-1} until failure was induced. The shear strength S_{xy} was calculated from the Eq. 3, which was proposed by Yoshihara and Yoshinobu (2014):

$$S_{xy} = 0.6F_{35} \tag{3}$$

where F_{35} is the tensile strength obtained from the tension test of the 35° OA specimen.

Results and discussion

There are significant differences between the values of τ_{xy}^{FEM} and $\tau_{\mathrm{xy}}^{\mathrm{EBT}}$ in the FEA results; therefore, the value of α, defined as $\tau_{\mathrm{xy}}^{\mathrm{FEM}}/\tau_{\mathrm{xy}}^{\mathrm{EBT}}$, was calculated along with the principal stress angle, defined as φ. Figure 4 shows the α value along the neutral axis corresponding to the location from the mid-span of the model/clearance length x/c. If elementary beam theory is applicable, the α value should be equal to 1. Because of the large deformation of the tab-free region, however, beam theory is not effective because v deviates from 1. When c=0, the α values obtained from the three paper models are different and >1. In contrast, they are <1 when the c value is >5 mm, and they increase as c increases. There was a concern that a significant stress concentration at the inner edge of the tab might induce failure at the inner edge. From the distribution of the α value, however, the stress concentration was effectively reduced when the c value was appropriately determined. In addition, the φ value in the tab-free region was approximately equal to 45°, so a pure shear stress condition was confirmed. Therefore, the shear stress at the tab-free region can be derived from the applied load using the α value.

To obtain the shear strength of the paper specimen, the value of $\bar{\alpha}$ was obtained by averaging the α values (Table 3). The table indicates that the $\bar{\alpha}$ values obtained from each paper are similar with each other in the same clearance length except for c=0. Using the $\bar{\alpha}$ value, the shear strength S_{xy} obtained from the AFPB test was calculated from the following equation:

$$S_{xy} = \frac{3P_{\max}}{4BW} \bullet \bar{\alpha} \tag{4}$$

where $P_{\max}$ is the maximum load. A comparison of the S_{xy} values determined from the AFPB and 35° OAT tests are presented in Figure 3. There are no significant differences between the shear strengths obtained from the MD and CD specimens for the AFPB test results. When c=0, the S_{xy} value obtained from the AFPB test is significantly greater than that obtained from the OAT test. When the c value is >5 mm, the S_{xy} values of the filter paper coincide well with those obtained from the off-axis tension test, whereas those of copy paper and sack paper are significantly lower than those obtained from the OAT test. This difference is due to the thinness of the material.

Figure 4 shows a photograph of the specimens after conducting the AFPB tests. When a pure shear stress occurs in a material, the principal stresses should be ±45°. Because of the negative principal stress, a localised buckling is easily induced, as shown in Figure 4, when the specimen is very thin. The oblique wrinkles in the copy paper and sack paper are due to localised buckling, whereas the failures are induced perpendicular to the wrinkles. This buckling can be easily induced under a small load, and the S_{xy} value obtained from the AFPB test is therefore lower than that obtained from the OAT test, where compressive stress does not occur. In contrast, the filter paper is thick enough to prevent the specimen from buckling, so the S_{xy}

Figure 4 Specimens after conducting the AFPB test.

value obtained by the AFPB test is close to that obtained from the OAT test. The shear strength is a material property that is essentially independent of the geometry of the material. Considering this principle, the conflict between the S_{xy} values obtained by these different methods must be reduced. When a pure shear load is applied to a thin paper, however, the localised buckling is not inevitably reduced. Therefore, it may be necessary to estimate the shear strength of paper according to the test methods, including the OAT, SS, and AFPB tests. Additionally, it may be necessary to compare the shear strengths obtained from different methods with each other.

Table 3 Average α values obtained from the finite element analysis (FEA).

Paper type	Average α values at clearance length c (mm)				
	0	5	10	15	20
Copy p. MD	1.17	0.70	0.72	0.76	0.79
Copy p. CD	1.18	0.70	0.74	0.78	0.81
Filter p. MD	6.39	0.72	0.74	0.77	0.80
Filter p. CD	6.39	0.72	0.75	0.79	0.82
Sack p. MD	1.73	0.69	0.71	0.74	0.77
Sack p. CD	1.74	0.67	0.74	0.78	0.82

MD, machine direction; CD, cross direction.

When c=5–10 mm, the dependence of the S_{xy} value on the clearance length is restricted for the papers examined in this study. In this range of clearance length, the $\bar{\alpha}$ value is approximately 0.72. Further research should be conducted to determine the appropriate $\bar{\alpha}$ value for various papers. Additionally, full-field displacement measurement methods including digital image correlation (DIC) technique may provide more detailed information on the shear properties of paper (Choi et al. 1991; Enomae 2007; Koerber et al. 2010; Xavier et al. 2007, 2009, 2013). These results do, however, show promise in determining the shear strength of paper through AFPB tests under a rather pure shear stress condition.

Conclusions

The IPSS of copy paper, filter paper, and sack paper was measured by an AFPB test, and the validity of the AFPB test was examined through a subsequent 35° OAT test and numerical analysis. The IPSS values obtained from the AFPB test for the copy paper and sack paper were lower than those obtained from the 35° OAT test because of localised buckling caused by negative principal stress. In contrast, the IPSS values of the filter paper obtained from the AFPB and OAT tests coincided well with each other when the clearance length was >5 mm, as buckling did not occur.

Acknowledgments: This work was supported in part by a Grant-in-Aid for Scientific Research (C) (No. 24580246) of the Japan Society for the Promotion of Science.

References

Azzi, V.D., Tsai, S.W. (1965) Anisotropic strength of composites. Exp. Mech. 5:283–288.

Choi, D., Thorpe, J.L., Hanna, R.B. (1991) Image analysis to measure strain in wood and paper. Wood Sci. Technol. 25:251–262.

Enomae, T. (2007) Application of image correlation technique to determination of in-plane deformation distribution of paper. J. Jpn. Soc. Nondest. Inspec. 56:561–566.

Fellers, C. (1977) Procedure for measuring the interlaminar shear properties of paper. Svensk Papperst. 3:89–93.

Heckers, W., Göttsching, L. (1980) Ein Verfahren zur Bestimmung der Scherfestigkeit in der Bahnebene von Papier und Karton. Das Papier 34:1–5.

Koerber, H., Xavier, J., Camanho, P.P. (2010) High strain rate characterisation of unidirectional carbon-epoxy IM7-8552 in transverse compression and in-plane shear using digital image correlation. Mech. Mater. 42:1004–1019.

Kubojima, Y., Yoshihara, H. Ohsaki, H., Ohta, M. (2000) Accuracy of shear properties of wood obtained by simplified Iosipescu shear test. J. Wood Sci. 46:279–283.

Norris, C.B. (1962) Strength of orthotropic materials subjected to combined stresses. Forest Prod. Lab. Rep. 1816:1–40.

Pan, N., Zhang, X. (1997) Shear strength of fibrous sheets: an experimental investigation. Textile Res. J. 67:593–600.

Waterhouse, J.F. (1984) The ultimate strength of paper. IPC Tech. Paper Ser. 146:1–35.

Wu, R.-Y., Stachurski, Z. (1984) Evaluation of the normal stress interaction parameter in the tensor polynomial strength theory for anisotropic materials. J. Compos. Mater. 18:456–463.

Xavier, J., Avril, S., Pierron, F., Morais, J. (2007) Novel experimental approach for longitudinal-radial stiffness characterisation of clear wood by a single test. Holzforschung 61:573–581.

Xavier, J., Avril, S., Pierron, F., Morais, J. (2009) Variation of transverse and shear stiffness properties of wood in a tree. Composites A 40:1953–1960.

Xavier, J., Belini, U., Pierron, F., Morais, J., Lousada, J., Tomazello, M. (2013) Characterisation of bending stiffness components of MDF panels from full-field slope measurements. Wood Sci. Technol. 47:423–441.

Yoshihara, H. (2009) Shear properties of wood measured by the asymmetric four-point bending test of notched specimen. Holzforschung 63:211–216.

Yoshihara, H. (2012) Interlaminar shear strength of medium-density fiberboard obtained from asymmetric four-point bending tests. Construct. Build. Mater. 34:11–15.

Yoshihara, H. (2013) Mode II critical stress intensity factor of medium-density fiberboard measured by asymmetric four-point bending tests and analyses of kink crack formation. BioResources 8:1771–1789.

Yoshihara, H., Kondo, H. (2013) Effect of specimen configuration and lamination construction on the measurement of the in-plane shear modulus of plywood obtained by the asymmetric four-point bending test. BioResources 8:3858–3868.

Yoshihara, H., Suzuki, A. (2005) Shear stress/shear strain relation of wood obtained by asymmetric four-point bending test of side-tapered specimen. J. Test. Eval. 33:55–60.

Yoshihara, H., Yoshinobu, M. (2014) Off-axis tensile strength and evaluation of the in-plane shear strength of paper. Holzforschung 68:583–590.

Yoshihara H., Kubojima, Y., Nagaoka, K., Ohta, M. (1998) Measurement of the shear modulus of wood by static bending tests. J. Wood Sci. 44:15–20.

Yoshihara, H., Ohsaki, H. Kubojima, Y. Ohta, M. (1999) Applicability of the Iosipescu shear test on the measurement of the shear properties of wood. J. Wood Sci. 45:24–29.